Vol. 480: 39–56, 2013
doi: 10.3354/meps10215

MARINE ECOLOGY PROGRESS SERIES
Mar Ecol Prog Ser

Published April 22

Second-order seasonal variability in diel vertical migration timing of euphausiids in a coastal inlet

Mei Sato[1,*], John F. Dower[2,1], Eric Kunze[3], Richard Dewey[1]

[1]School of Earth and Ocean Sciences, University of Victoria, Victoria, British Columbia V8P 5C2, Canada
[2]Department of Biology, University of Victoria, Victoria, British Columbia V8P 5C2, Canada
[3]Applied Physics Laboratory, University of Washington, Seattle, Washington 98105-6698, USA

ABSTRACT: Variability in the diel vertical migration timing of euphausiids in Saanich Inlet, British Columbia, Canada, is quantified using 2 yr of echosounder data from a cabled observatory. The continuous and high-resolution nature of the observations allows examination of second-order seasonal variability in migration timing relative to civil twilight times. Early dusk ascent and late dawn descent occur during spring–fall, while late dusk ascent and early dawn descent occur during winter. Ascent timing appears to be regulated by (1) light availability at the daytime depth of the euphausiids, which is modulated by phytoplankton bloom shadowing, and (2) euphausiid size-dependent visual predation risk. Because (1) does not apply at dawn, descent timing appears to be regulated by (2). During the pre-spawning period, higher energy demand for reproduction may cause earlier dusk ascent and later dawn descent to maximize energy gain, even with larger body size. Instead of the traditional view of diel vertical migration timing, correlated solely with civil twilight, our data suggest that euphausiids also adapt their migration timing to accommodate changes in environmental cues as well as their growth.

KEY WORDS: Diel vertical migration · Euphausiids · Variability · Echosounder · Time-series

INTRODUCTION

Many planktonic species migrate away from food-rich surface waters during the day to avoid visual predators (Zaret & Suffern 1976). Quantifying the variability in such diel vertical migration is essential to understand predator–prey interactions and assess the least-known component of the biological pump (Steinberg et al. 2000). Euphausiids play a key role in pelagic food webs, being a grazer on phytoplankton, a predator on microzooplankton, and a key prey item for invertebrate, fish and marine mammals (Mauchline 1980, Mackas et al. 1997). Variations in migration timing can influence encounters with both predators and food, so they are a key factor for survival. Diel vertical migration also serves as a vector connecting deep-water and pelagic communities by actively transporting carbon and nutrients from the surface to deep waters (Longhurst & Harrison 1988). However, its global contribution to biogeochemical cycles remains unresolved.

If diel vertical migration behavior is primarily a consequence of the conflicting requirements of feeding and predator avoidance (Bollens & Frost 1989), the time at which organisms migrate between deep and surface waters should reflect this trade-off. Light has long been known to be the dominant factor controlling the timing of diel vertical migration (Forward 1988). Since migrating zooplankton typically reside at depth during the day, the light intensity that they experience can vary with the attenuation and spectral characteristics of light, which, in turn, are affected by the presence of dissolved and suspended material (Hulburt 1945, Tyler 1975). In addition to the ambient light level, food availability and predator density are also thought to be factors affecting diel

*Email: meisato@uvic.ca

vertical migration. According to the hunger-satiation hypothesis (Pearre 2003), diel vertical migration is asynchronous within the population; animals leave the surface waters during the night when they are satiated, and may go back for a second meal before dawn after digesting their early-night meal (e.g. Simard et al. 1985, Sourisseau et al. 2008). Differences in predation risk between and within species also cause variations in migration timing (e.g. De Robertis et al. 2000, Tarling et al. 2001).

Although these various factors have been studied in the lab and over short periods in the field, long-term *in situ* observations of diel vertical migrations remain few. Previous studies based on long time-series have shown changes in migration timing due to the seasonal shift in daylight length (Tarling 2003, Lorke et al. 2004, Jiang et al. 2007) at first order. However, second-order variability (variability in migration timing relative to civil twilight times) has received little attention due to low sampling resolution and short record length. One of the few examples is consideration of variations in migration timing with euphausiid body size (De Robertis et al. 2000). High sampling resolution and long time-series are essential for understanding behavior driven by factors whose relative importance can change temporally. For example, Sato & Jumars (2008) demonstrated the value of high temporal and spatial sampling resolution by showing a shift in the dominant rhythm of mysid emergence patterns from diel in summer to semidiurnal in fall.

If diel vertical migration is a trade-off between energy gain and mortality risk (Bollens & Frost 1989), then migration timing should not be tied solely to civil twilight times. Rather, variability in migration timing due to light intensity, food availability, predator density and predation risk should be expected. The goal of this study is to examine second-order variability in migration timing relative to civil twilight, and to identify the factors responsible for this variability. Here, we present data from a 2-yr 200-kHz echosounder time-series collected in Saanich Inlet by the Victoria Experimental Network Under the Sea (VENUS) cabled observatory.

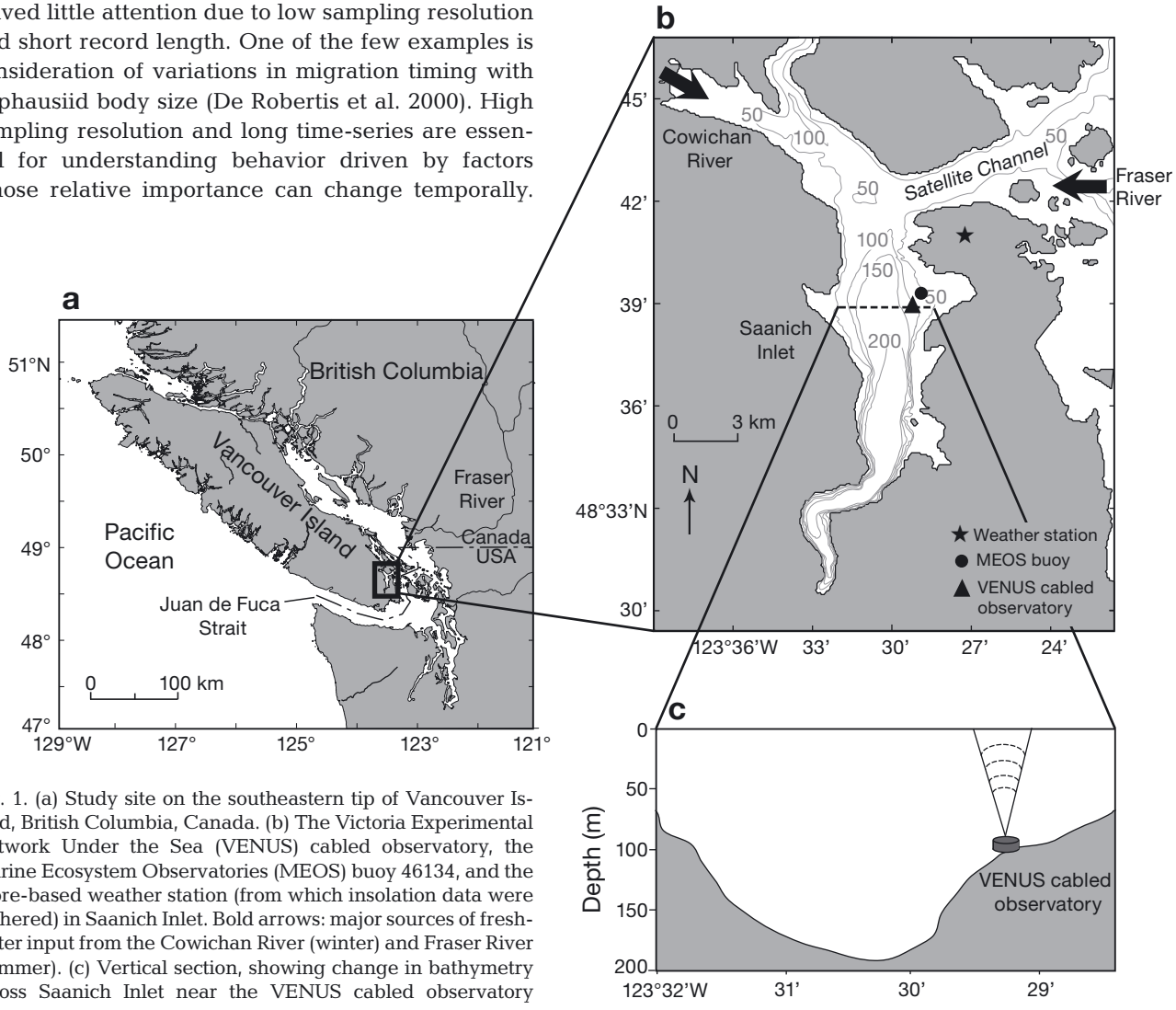

Fig. 1. (a) Study site on the southeastern tip of Vancouver Island, British Columbia, Canada. (b) The Victoria Experimental Network Under the Sea (VENUS) cabled observatory, the Marine Ecosystem Observatories (MEOS) buoy 46134, and the shore-based weather station (from which insolation data were gathered) in Saanich Inlet. Bold arrows: major sources of freshwater input from the Cowichan River (winter) and Fraser River (summer). (c) Vertical section, showing change in bathymetry across Saanich Inlet near the VENUS cabled observatory

MATERIALS AND METHODS

Study site

Data were collected in Saanich Inlet (48° 39.1′ N, 123° 29.2′ W), British Columbia, Canada, from June 2008 to May 2010 (Fig. 1). Saanich Inlet is a fjord, with a 75 m sill at its mouth and maximum depths >200 m (Herlinveaux 1962). It is a reverse estuary with its major supply of freshwater outside the inlet mouth. The Cowichan River in winter and the Fraser River freshet in summer produce a year-round stabilizing salinity gradient in the upper water column. Wind and tidal forcing in Saanich Inlet are generally weak (Gargett et al. 2003). The estuarine circulation is normally too weak to permit flushing of deeper waters below the sill, so that a secondary halocline exists at sill depth (Herlinveaux 1962). High primary production (~475 g C m^{-2} yr^{-1}) combined with infrequent deep-water replenishment contribute to the formation of deep-water anoxia during much of the year (Timothy & Soon 2001, Grundle et al. 2009). There are typically 2 renewal events per year in Saanich Inlet where dense oxygenated waters enter the mouth at the sill depth, shoaling the deep anoxic waters upward: (1) deep-water renewal (below the sill depth but not reaching the bottom) during spring and (2) bottom-water renewal during fall (Anderson & Devol 1973, Manning et al. 2010). The oxycline plays a major role in Saanich Inlet in determining the daytime depth of the scattering layer, posing a physiological barrier for euphausiids (Pieper 1971, Devol 1981, Mackie & Mills 1983).

Potential acoustic scatterers of a 200-kHz echosounder

Year-round dominance of euphausiids in Saanich Inlet is supported by previous studies through optical images (Jaffe et al. 1998), visual observations (Mackie & Mills 1983), and sampling using a 10-net MOCNESS (Multiple Opening/Closing Net and Environmental Sensing System; De Robertis 2001). Densities of euphausiids within the scattering layers range from 10 to 10 000 individuals (ind.) m^{-3} (Bary et al. 1962, Bary 1966, Pieper 1971, Mackie & Mills 1983), accounting for ~70% of the daytime and ~76% of the night-time scattering layers based on the forward problem predictions of acoustic scatterers (Holliday & Pieper 1995, De Robertis 2002). *Euphausia pacifica* is the most abundant euphausiid throughout the year, constituting 77 to 100% of all euphausiids followed by *Thysanoessa spinifera* and *T. raschii* (Bary et al. 1962, Pieper 1971, De Robertis 2001). *E. pacifica* live 1 to 2 yr (Tanasichuk 1998) with their main spawning period from early May to mid-July, coinciding closely with the periods of higher phytoplankton abundance (Parsons et al. 1967, Heath 1977).

The gammarid amphipod *Orchomene obtusus* is also abundant in Saanich Inlet (Bary et al. 1962, De Robertis 2001), but resides at 100 to 125 m depth and does not migrate (De Robertis et al. 2000, De Robertis 2001). Since the present study focuses on diel vertical migration behavior in the upper 50 m of the water column, *O. obtusus* is unlikely to contribute to the major acoustic scatterers. Low biomass of copepods (Bary et al. 1962) and their low target strength (TS) values at 200 kHz due to their small body size (Trevorrow 2005) suggest that their contribution to volume backscattering strength (S_v) is also minimal. Decapods, mysids, shrimps, physonectid siphonophores, gastropods, hydromedusae, ctenophores, chaetognaths and cephalopods have been observed in previous studies, but their rare occurrence and low density in scattering layers suggest insignificance as acoustic scatterers (Bary et al. 1962, Pieper 1971, Mackie & Mills 1983, De Robertis 2001). Although the thecosome pteropod *Limacina helicina* and the gas-filled pneumatophores of siphonophores are strong acoustic targets (Stanton et al. 1994), scattering model calculations of *L. helicina*, which are <2 mm in diameter, indicated that their contribution to echoes is not significant at 445 kHz (De Robertis 2001). Since theoretical TS value of the pteropods is predicted to be lower at 200 kHz than at 445 kHz (Stanton et al. 1994), their contribution is not significant at 200 kHz either. The density of physonectid siphonophore in Saanich Inlet is not known. In the present study, we assumed that their contributions to S_v were minimal.

Other possible biological acoustic targets include Pacific herring *Clupea pallasi*, hake *Merluccius productus*, walleye pollock *Theragra chalcogramma*, rockfish *Sebastodes* spp., myctophids *Lampanyctus leucopsarus*, eulachon *Thaleichthys pacificus*, smooth-tongue *Leuroglossus stilbius*, and spiny dogfish *Squalus acanthias* (Bary et al. 1962, Bary 1966, Pieper 1971, De Robertis 2002). Among these fish, herring and young hake are the principal species associated with the scattering layers (Bary 1966). Based on the minimal effect of fish schools on migration timing detection (see 'Data analysis: Application of threshold' below), they are not likely to affect estimates of

euphausiid migration timing, which is the focus of this study. Sediments and bubbles are unlikely to contribute to the backscattering observed in our record. Given the weak tidal forcing in Saanich Inlet (5 to 10 cm s^{-1}), sediments are unlikely to be stirred >2 m above bottom (mab). Bubbles are largely confined to the surface layer under breaking waves, which are not common in Saanich Inlet due to shelter from prevailing winds.

Identification of acoustic scatterers

Sampling of the zooplankton community was carried out for ~3 h near the VENUS cabled observatory around sunset on 15 April, 10 June, 15 July 2010, and sunrise on 14 October, 16 December 2011, and 9 February 2012 to confirm dominance of euphausiids in the scattering layer. A Tucker trawl (1 m^2 mouth opening when towed at 45°, 1 mm mesh size) equipped with a double-release mechanism (Ocean Test Equipment) was towed at ~80, 40 and 10 m depths to compare the species composition inside and outside the diel migratory scattering layer. These depths were chosen to capture the scattering layer located at the daytime depth before the migration started, mid-depth during the migration, and near the surface after the upward migration was completed. Samples from outside the scattering layer were collected by towing at the above depths starting before the migrating scattering layer crossed and continuing after the layer had crossed these depths. A pressure sensor (Minilog-TD; AMIRIX Systems) on the Tucker trawl monitored tow depth. Each sample consisted of ~5 min horizontal tow at ~1 m s^{-1}. Samples were fixed in 5% formalin on deck, and displacement volume determined ashore after removal of jellyfish because they are weak acoustic targets compared to non-gelatinous zooplankton (Stanton et al. 1996). Animals were subsequently sorted, counted, and the total lengths of dominant euphausiids (tip of eye to tip of telson) measured under a dissecting microscope. Juvenile euphausiids were not identified in species level due to the difficulty in recognizing developing characteristics. Since a flow meter could not be mounted in the net mouth due to the mechanical limitations of using a double-release mechanism, abundance and displacement volume were normalized to 5 min tows to compare between samples. Copepods and fish were not collected in representative numbers by the 1 mm mesh of the Tucker trawl but, as already argued, are unlikely to contribute to migration timing detection.

VENUS instruments

Diel vertical migration of zooplankton was monitored with an upward-looking 200-kHz echosounder (Acoustic Water Column Profiler; ASL Environmental Sciences) mounted on a metal frame at 100 m depth (~2 mab) above the oxycline throughout most of the year. Therefore, we could not quantify the seasonal change in daytime depth of the scattering layer in this study. A CTD (SBE 16plus; Sea-Bird Electronics) was deployed on the same frame. All instruments were linked to the VENUS cabled observatory (http://venus.uvic.ca) and were serviced and cleaned twice a year to remove biofouling.

Backscattered acoustic signals from particles in the water column were digitized (8-bit resolution) into 12.5-cm depth bins, with a sampling interval of 2 s, pulse duration of 300 µs and beam width of 8°, then converted to S_v using the standard sonar equation (e.g. Urick 1983):

$$S_v = 20\log_{10} N_r + 20\log_{10} r + 2\alpha r - \mathrm{SL} - \mathrm{OCV} - G - 10\log_{10}\left(\frac{c\tau\psi}{2}\right) \quad (1)$$

where N_r is received signal output by the 8-bit A/D converter between 0 and 255, r the range of the target sensed by the transducer (m), α the absorption coefficient of the medium (dB m^{-1}), SL the source level of the transmitted signal (dB re 1 µPa at 1 m), OCV the transducer receiving response (dB re 1 V per 1 µPa), G the time-varying gain of the echosounder (dB), c the sound speed (m s^{-1}), τ the pulse duration (s), and ψ the equivalent beam angle (sr). The range of S_v detectable was approx. −80 to −43 dB re 1 m^{-1} at 50 m range and −72 to −41 dB re 1 m^{-1} at 100 m range. The resolution depends on the signal strength, varying from 0.03 to 1.9 dB at 50 m range and 0.03 to 1.2 dB at 100 m range. To ensure continuous time-series data, 2 identical echosounders (AWCP 1007, 1009) were deployed alternately.

Calibrations

Both echosounders were calibrated using a 38.1 mm diameter tungsten carbide sphere as prescribed by Vagle et al. (1996). Calibrations were conducted at the buoy of the Ocean Technology Test Bed, an underwater engineering laboratory operated by the University of Victoria in Saanich Inlet (Proctor et al. 2007), on 9 February 2010 for AWCP 1007, and 31 January 2011 for AWCP 1009. Due to the technical difficulties in calibrating bottom-mounted echo-

sounders at the operating depth of 100 m, calibrations were conducted near the surface. The transducer was mounted at ~0.7 m depth facing downward, and calibration measurements were conducted at 22.66, 24.69, 30.76 and 36.83 m range for AWCP 1007, and 19.46, 21.48, 23.49, 25.53, 30.46 and 35.28 m range for AWCP 1009 to ensure calibration in the far field. On average, the mean adjustment needed in G was −0.34 dB for AWCP 1007, and −0.38 dB for AWCP 1009. Since the measured TS values were within 0.4 dB of the theoretical TS and depth dependency of transducer sensitivity could affect the calibration results (Ona 1999), no correction was applied to G in the present study (for more details of the calibration methods and associated results, see Appendix 1).

Additional data

Chlorophyll *a* concentration was monitored hourly by a WET Labs WETStar fluorometer deployed at 8 m depth on the Marine Ecosystem Observatories (MEOS) buoy 46134 (48° 39.6′ N, 123° 28.8′ W) (Fig. 1b). Chlorophyll *a* concentration, estimated using factory calibration values, was provided by J. Gower (pers. comm.; Gower et al. 1999, Gower 2001). The fluorometer was cleaned once a month to remove biofouling. Insolation data monitored at Deep Cove Elementary School (48° 40.8′ N, 123° 27.4′ W), ~4 km northeast of the study site (Fig. 1b), were obtained through the University of Victoria's school-based weather station network (www.victoriaweather.ca). Times of sunrise, sunset and civil twilight (sun zenith angle = 96°) for the study site were obtained from the United States Naval Observatory (http://aa.usno.navy.mil/data/).

Vertical profiles of fluorescence and photosynthetically available radiation (PAR; 400–700 nm) were measured near the VENUS cabled observatory using a WET Labs WETStar fluorometer and a Biospherical Instruments QSP-200L sensor, respectively. These data were analyzed to characterize the effect of phytoplankton blooms on underwater light intensity. Data were collected on 3 d in January (21 January 2009, 25 January 2010, and 25 January 2011), and 2 d in June (9 June 2010 and 10 June 2011) with 1 vertical cast per day whose sampling time varied between 10:11 and 14:10 PST. Since the spectral sensitivity of euphausiids has a narrower peak at 480–490 nm (Frank & Widder 1999, Widder & Frank 2001), our PAR data overestimate the true irradiance value available to the euphausiid eye.

To characterize vertical and seasonal variability of sound speed and absorption coefficient, CTD (SBE 19plus; Sea-Bird Electronics) profiles collected near the VENUS cabled observatory during January, May, June and July 2007–2011 were examined. Each month contained 2 to 7 vertical profiles.

Data processing

Two years (June 2008 to May 2010) of echosounder profile time-series were analyzed. Data gaps (2.6% of all data) due to mechanical problems and maintenance cruises were linearly interpolated to form a continuous data set. Based on the mean temperature (8.8°C) and Absolute Salinity (31.0 g kg^{-1}) measured by the CTD at 100 m depth for 2 yr, a constant sound speed of 1482 m s^{-1} and absorption coefficient of 0.05 dB m^{-1} were applied to calculate S_v throughout the water column. Based on seasonal and depth variations in sound speed of <1%, uncertainties in S_v, range and bin size were minimal. The use of a constant absorption coefficient results in <0.5 dB re 1 m^{-1} error in S_v at 100 m range. Raw S_v values were averaged into 1-min × 1-m bins. The detected ocean surface was used as a reference for analysis of migration timing and speed (see 'Data analysis: Effect of reference point' below). Time-series of fluorometer data measured hourly from the MEOS buoy were averaged over 1 d to be consistent with the number of occurrences of diel vertical migration.

3D data cube concept

The 2-yr echosounder time-series sampled every 2 s with 12.5-cm depth bins generated ~60 GB data. Analysis of such large datasets can be challenging. To deal with this problem, we utilize the data cube concept (Jiang et al. 2007, Sourisseau et al. 2008, Borstad et al. 2010, Cisewski et al. 2010) whereby echosounder data can be imaged in time-of-day × day × depth (Fig. 2a). By slicing this data cube vertically or horizontally, different aspects of diel vertical migration can be examined. To center the nocturnal diel vertical migration, each day begins at 12:00 PST (local noon) and ends at 12:00 PST of the following day. The first day in the time-series is 1 June 2008 and the last 1 June 2010. The cube was truncated at 3 m depth to present variation in ascent and descent timings of diel vertical migration without contamination by the surface. The seasonal variation in diel vertical migration regulated by the seasonal shift in day-

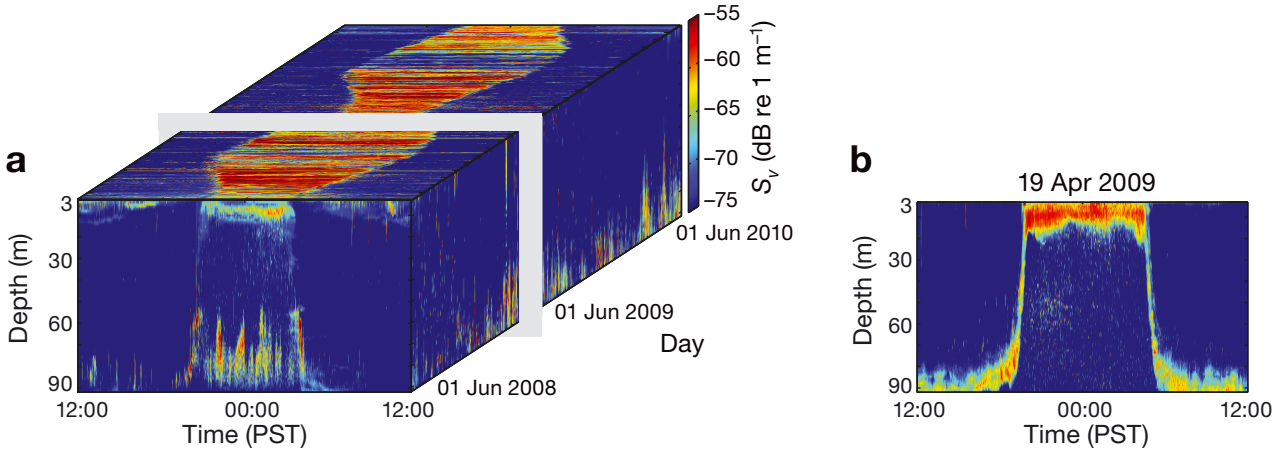

Fig. 2. (a) Time-series (2 yr) of volume backscattering strength (S_v) (1-min × 1-m bin averages), visualized as a 3D data cube: time-of-day × day × depth. Hourglass shape on top surface of cube shows first-order variability, which is the seasonal variation in diel vertical migration regulated by seasonal shift in daylight length. (b) Example of nocturnal diel vertical migration with a single scattering layer, corresponding to the vertical slice of the 3D data cube shown in (a)

light length is evident as an hourglass shape on the top surface of the cube (Fig. 2a). A vertical slice parallel to the *xz* plane shows the diel vertical migration pattern on 19 April 2009 (Fig. 2b). This pattern represents typical nocturnal diel vertical migration: upward movement of the scattering layer towards the surface at dusk and downward movement to deeper waters at dawn. Examples of more complicated scattering layer patterns are presented in the Discussion.

Data analysis

Migration timing

Using the acoustic sea surface as a reference, S_v were further smoothed by taking 11-min running × 5-m bin averages. Daily variability of S_v at 8 m depth, corresponding to the horizontal slice of the 3D data cube in Fig. 3a, was used to detect migration timing; S_v within the upper 20 m gives a similar pattern as that at 8 m depth, indicating that S_v at 8 m depth is representative of near-surface conditions. Differences of S_v [$\Delta S_v = S_v(t + \Delta t) - S_v(t)$, with time lag Δt = 20 min] were calculated to show the timing of increase/decrease in ΔS_v. Various Δt values were tested for estimating migration timing. By visually inspecting how well the estimated migration timing captured the migration timing in echograms, we settled on Δt = 20 min to calculate differences of S_v. Timing of diel vertical migration was estimated by detecting the maximum and minimum values of ΔS_v. The presence of non-migratory scatterers near the surface can contaminate migration timing detection. Based on visual examination, 35% of ascent and 29% of descent migration timings resulted in detection of such non-migratory scatterers. However, removal of those data points does not change the pattern of seasonally varying migration timing.

Detected migration timing was compared with the times of civil twilight to examine seasonal variability in ascent and descent migration timings. We also examined the migration timing relative to sunset and sunrise to find the effect of reference times. Seasonal variations in migration timing lags differ by <1 min between the 2 reference times. Since civil twilight times match migration timings more closely than sunset and sunrise times, civil twilight was used as a reference point in the present study (e.g. Blaxter 1973). Periodicities of variability in migration timing were determined by estimating the power spectral density (describing how the power of a signal is distributed with frequency).

Migration speed

In order to maintain the relatively high vertical resolution required to estimate migration speed, S_v were further smoothed by taking 11-min running × 2-m bin averages. The lag in migration timings between 19 and 50 m depths was used to estimate migration speed for each day. These depths were chosen to avoid the nearly exponential ascent and descent curves of the scattering layer in deep waters (Fig. 2b), and to include nocturnal sub-surface scattering lay-

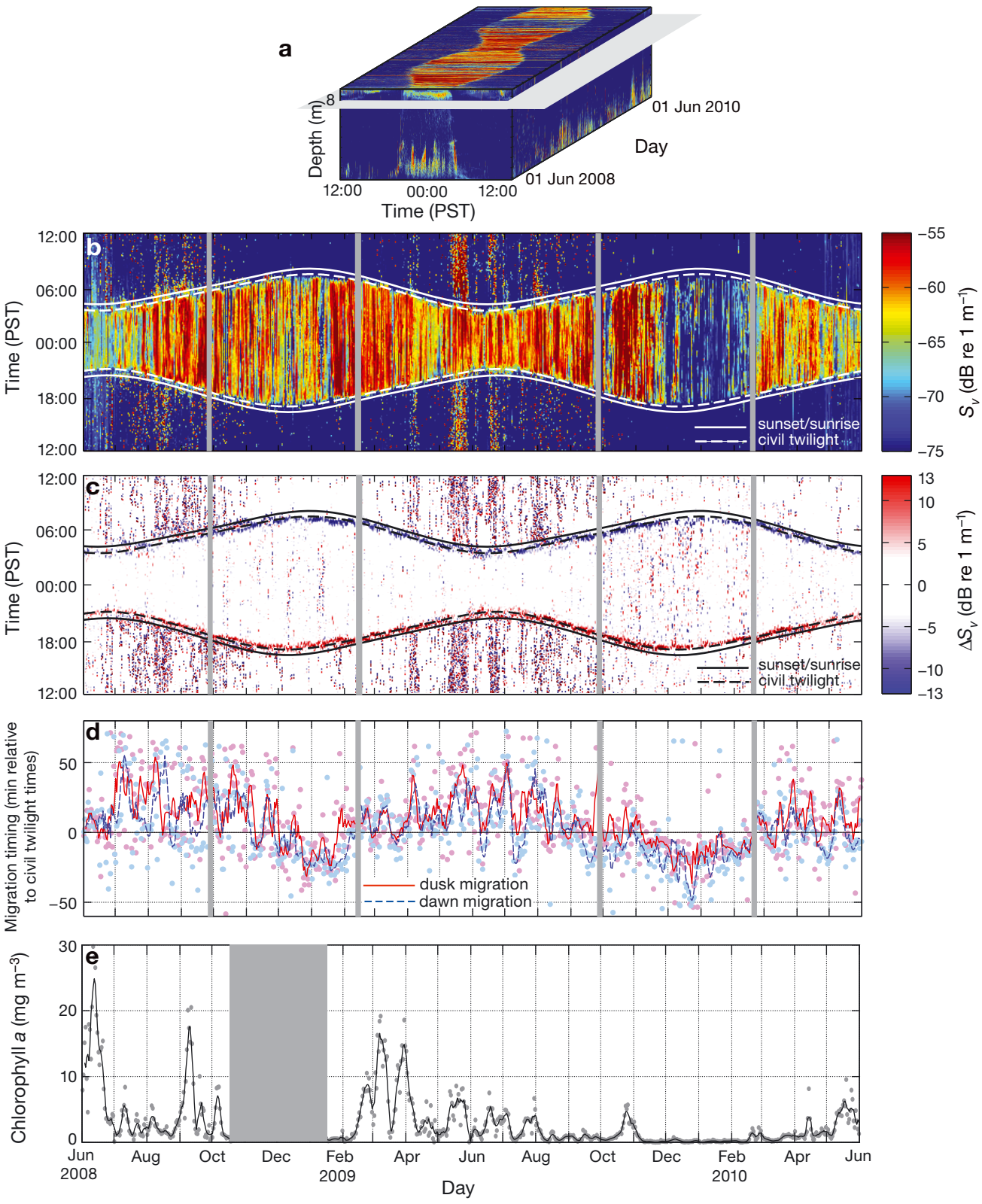

Fig. 3. (a) Time-series (2 yr) of volume backscattering strength (S_v) (1-min × 1-m bin averages) in 3D data cube, with a horizontal slice at 8 m depth. Daily variability of (b) S_v (11-min running × 5-m bin averages), and (c) 20-min difference of S_v: $\Delta S_v = S_v(t + \Delta t) - S_v(t)$, with time lag Δt = 20 min, at 8 m depth. (d) Timing of diel vertical migration relative to civil twilight times. Positive values: migration timing in min before civil twilight time for dusk ascent migration, and after civil twilight time for dawn descent migration. (e) Time-series of chl *a* concentration at 8 m depth. (d,e) Curves: 5 d running averages to remove day-to-day scatter. Data gaps (gray vertical bars) are due to maintenance cruises or mechanical failure of instruments

ers that were occasionally located at ~20 m depth. Owing to the differences in variance, Welch's *t*-test was used to test the null hypotheses of no differences in mean lag time among seasons assuming normal distributions.

Effect of reference point

Particle movement, as detected by echosounders, can be affected by vertical tidal motion. Therefore, the effect of choosing surface vs. bottom referencing on the migration timing analysis was examined. Spectral analysis of migration timing at 8 m depth, based on the 2-m bin-averaged bottom-referenced data, showed tidal components, indicating particle movement due to tidal heaving. Tidal surface displacements in Saanich Inlet vary from 2 to 3 m over the spring-neap cycle based on the VENUS pressure record. In order to avoid tidal effects on migration timing analysis near the surface, surface-referenced data smoothed over 11-min running × 5-m bin averages were used (see 'Data analysis: Migration timing' above). Spectral analysis of migration timing at 19 and 50 m depths showed no apparent tidal components, regardless of the reference point. This spectral characteristic suggests little effect of tidal displacements on migration timing at these depths.

Application of threshold

The presence of fish in our single-frequency echosounder data can be recognized as a plume shape for fish schools and a crescent-moon shape for individual fish. The potential effect of fish presence on migration timing detection was examined by applying an upper threshold in S_v (1-min × 1-m bin averages) to remove fish schools from the acoustic time-series. A representative probability density function of S_v in the presence of both the zooplankton scattering layer and fish schools showed bi-modal characteristics with peaks located at approx. −70 and −50 dB re 1 m^{-1}. Therefore, an upper threshold of −60 dB re 1 m^{-1} was chosen to filter out fish school echoes. Individual fish targets cannot be entirely extracted by thresholding; assuming that the TS of a 15-mm euphausiid is −79.8 dB re 1 m^2 at 200 kHz (Trevorrow 2005) and that their densities within scattering layers in Saanich Inlet range from 10 to 10 000 ind. m^{-3} (Bary et al. 1962, Bary 1966, Pieper 1971, Mackie & Mills 1983), the expected S_v varies from −69.8 to −39.8 dB re 1 m^{-1}, which overlaps with the detected S_v of individual fish. This overlap suggests that a −60 dB re 1 m^{-1} threshold would remove S_v due to the scattering layer comprised of euphausiids, in addition to fish schools. Given these limitations, a threshold approach could not be used to quantify predator density. A lower threshold to remove noise was not applied because its application masks the weak diel vertical migration patterns during December 2009 to February 2010. Detected migration timings were indistinguishable from those timings without thresholds. Thus, the results below are presented without an upper threshold as well.

RESULTS

Species composition from Tucker trawl samples

Euphausiids, shrimp larvae, amphipods and chaetognaths accounted for most of the zooplankton collected in the migratory scattering layers. Euphausiids (mostly *Euphausia pacifica*) were the dominant acoustic scatterers throughout the year, constituting >84% of individuals within the scattering layer in April (>78% of total displacement volume), 91% in June (64%), 59% in July 2010 (67%), 98% in October (86%), 90% in December 2011 (99%), and 83% in February 2012 (78%). Fewer organisms were captured outside of the scattering layers, with very few euphausiids. Displacement volumes outside the scattering layers were 9 to 32% of those inside the scattering layers. Although the period of Tucker trawl sampling did not exactly match that of the echosounder time-series, the numerical and displacement volume dominance of *E. pacifica* in the scattering layers in Saanich Inlet is well-supported by numerous previous studies (e.g. Bary et al. 1962, Mackie & Mills 1983, De Robertis et al. 2000). Given its dominance in the scattering layers, and that thresholding for fish schools did not affect migration timings, we hereafter assume that *E. pacifica* dominates diel vertical migration signals throughout the year.

Diel vertical migration timing

Nocturnal diel vertical migration, defined as a significantly higher S_v near the surface at night than during the day, occurs throughout the record (Fig. 3b), the only exception being low nocturnal S_v during December 2009 to February 2010. First-order variability is characterized by the seasonal change in migration timing associated with the seasonal shift in

daylight length; scattering layers remain near the surface at night longer during winter than summer (Fig. 3b). Migration timing is closely related to civil twilight times (Fig. 3b), corresponding to the maximum and minimum values of ΔS_v (Fig. 3c).

Superimposed on this light-regulated pattern is seasonal and intraseasonal variability in migration timing relative to civil twilight times. Seasonal variability is characterized by the difference in offset between civil twilight and dusk ascent/dawn descent migration timings (Fig. 3d). Referenced to civil twilight times, early dusk ascent and late dawn descent occur during spring–fall, while late dusk ascent and early dawn descent are observed during winter (Fig. 4). There is a positive correlation ($r = 0.71$, $p < 0.0001$) between dusk ascent and dawn descent migration timings relative to civil twilight times (Fig. 5a). On average, dusk ascent occurs 14.3 ± 14.1 min before civil twilight during spring–fall, and 8.6 ± 11.9 min after civil twilight during winter, while dawn descent occurs 8.2 ± 15.1 min after civil twilight during spring–fall, and 15.2 ± 12.4 min before civil twilight during winter. Spectral analysis of the 2-yr time-series of migration timing shows a clear peak at an annual period for both dusk ascent and dawn descent migration timings (Fig. 5b).

Intraseasonal (<100 d) variability in the timing of the dusk ascent and dawn descent is of similar amplitude, with fluctuations in both signals being larger during summer than winter (Fig. 3d). However, there is no consistent correlation between dusk ascent and dawn descent migration timings on these timescales. Power spectral densities at intraseasonal timescales are nearly flat and have no significant peaks (Fig. 5b). Non-migratory scatterers are often detected during summer–fall but intraseasonal variability remains after removal of these data points, though interpretation becomes difficult because of increased data gaps. Because a Fourier transform smears out any detailed information on the changing processes, the intraseasonal variability will not be considered further in this study.

Factors affecting diel vertical migration timing

Shadow effect of phytoplankton

Light intensity at depth is modified by dissolved and suspended material in the water column as well as seasonal change in insolation. Insolation at Saanich Inlet varies seasonally by over an order of magnitude, from a winter minimum of <50 W m^{-2} to a summer maximum of ~1000 W m^{-2}. However, despite the stronger insolation in summer, PAR deeper than 10 m depth is weaker in June than January (Fig. 6a) because it is below the depth of the chlorophyll maximum during phytoplankton blooms

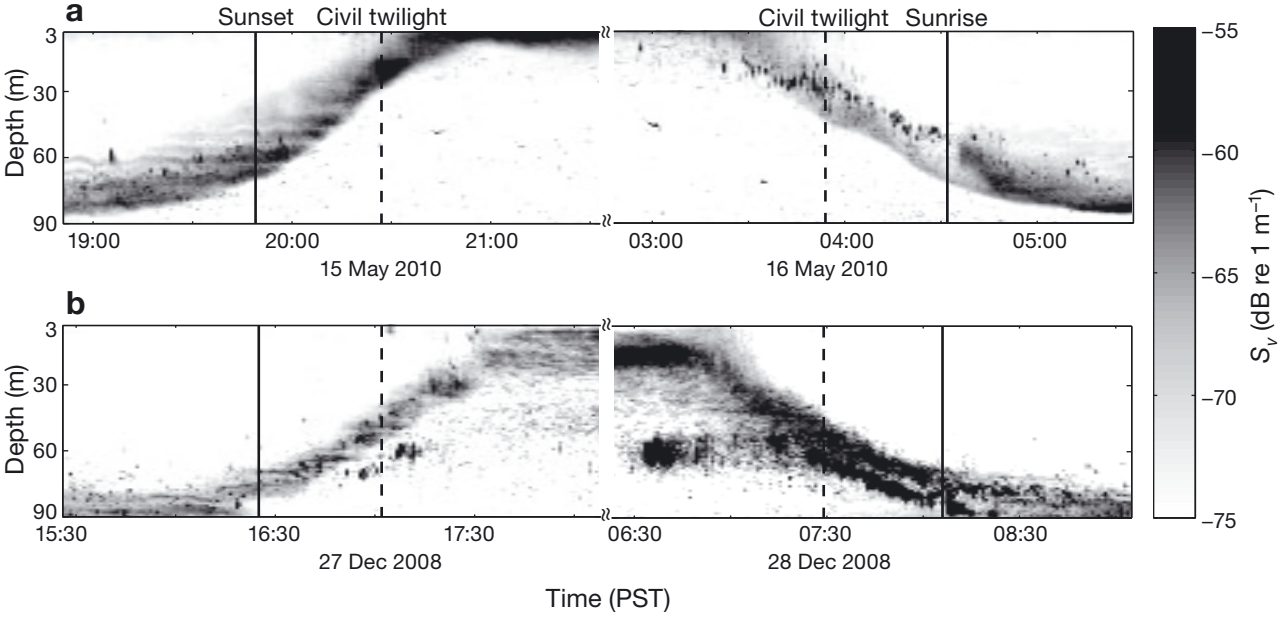

Fig. 4. Examples of second-order seasonal variability in dusk ascent and dawn descent migration timings during (a) summer and (b) winter. The lag between civil twilight times and dusk ascent/dawn descent migration timings near the surface is larger during winter than spring–fall; early dusk ascent and late dawn descent occur during spring–fall, while late dusk ascent and early dawn descent are observed during winter

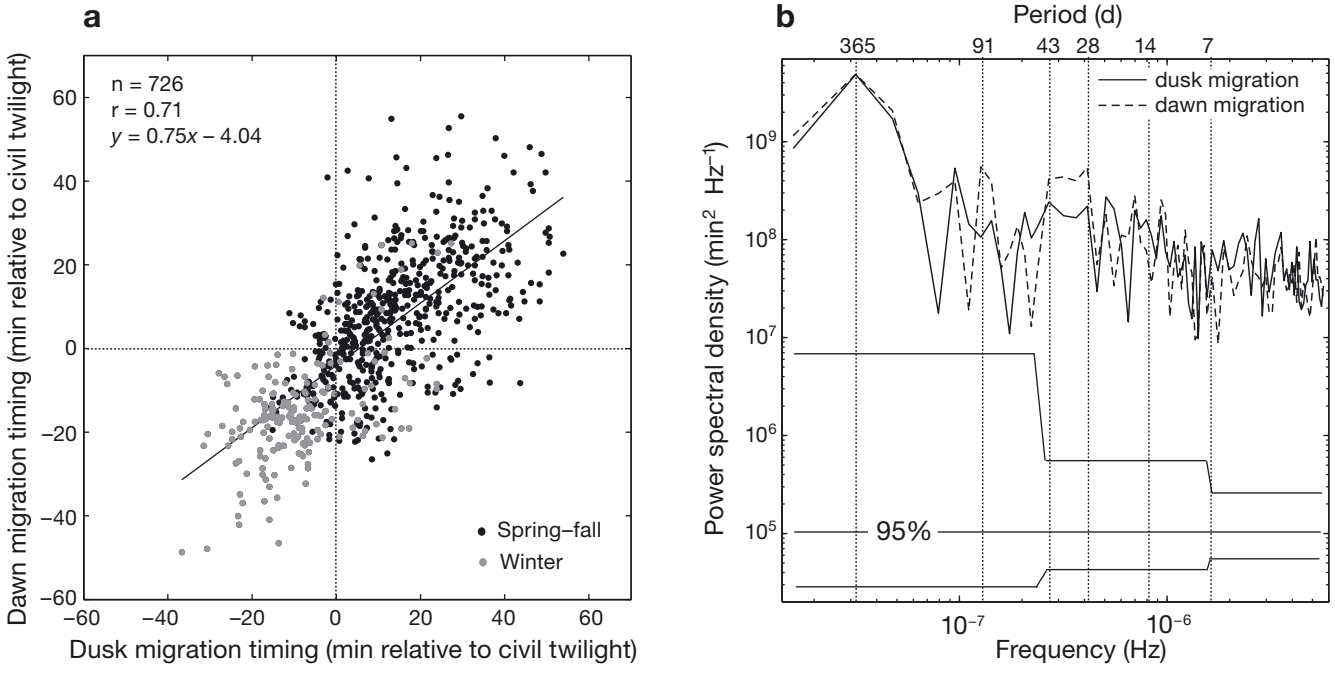

Fig. 5. (a) Scatterplot of dusk ascent vs. dawn descent migration timings at 8 m depth with 5-d running averages for the 2-yr time-series. Positive values: migration timing in min before civil twilight time for dusk ascent migration, and after civil twilight time for dawn descent migration. (b) Power spectral density of dusk ascent and dawn descent migration timings at 8 m depth for the 2-yr time-series. Lines: 95% CI

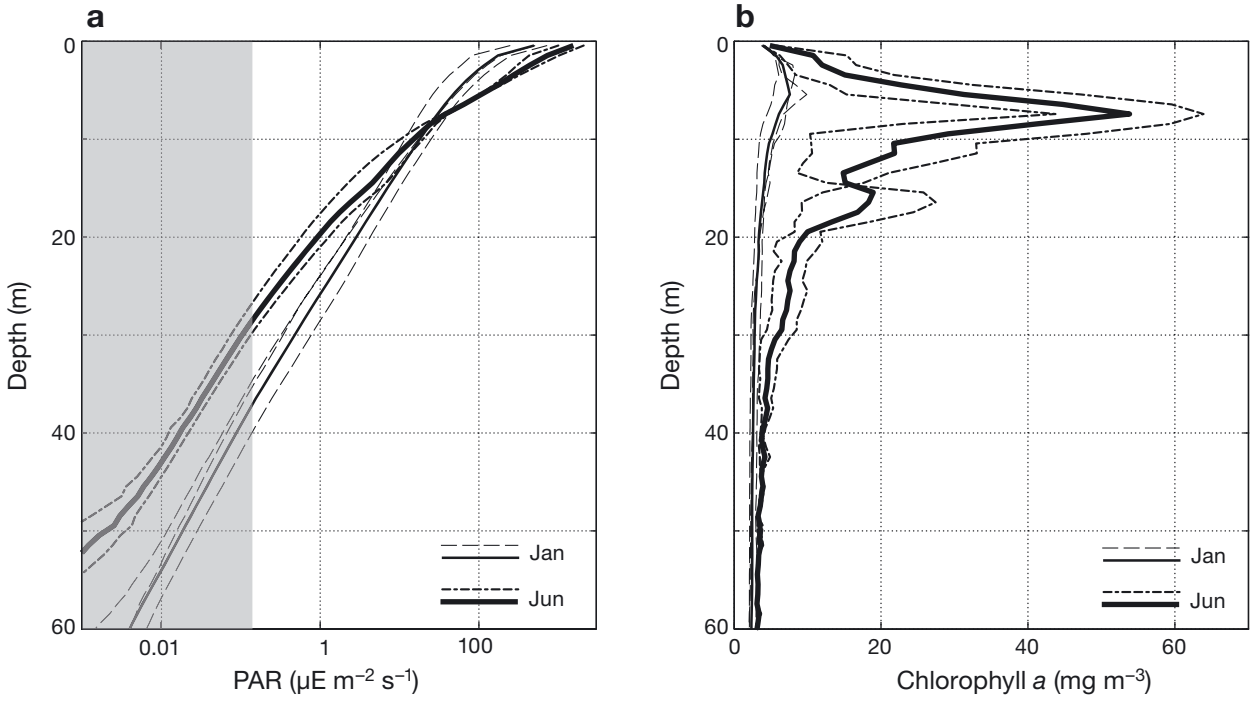

Fig. 6. Vertical profiles of daytime (a) photosynthetically available radiation (PAR) and (b) chl *a* concentration in Saanich Inlet during January (21 January 2009, 25 January 2010, 25 January 2011) and June (9 June 2010, 10 June 2011). Data averaged into 1-m bins. Vertical profiles collected each day (dashed lines) and monthly-averaged (solid lines). Gray: range of values below manufacturer's dynamic range

(Fig. 6b). Phytoplankton blooms in Saanich Inlet occur in spring–fall, with chl *a* concentrations often exceeding 15 mg m^{-3} at 8 m depth (Fig. 3e).

Body size of euphausiids

Juvenile euphausiids dominate the Saanich population in summer while adults dominate in winter–spring. The size distribution of euphausiids collected from the surface scattering layers in Saanich Inlet shows a seasonal shift in average body length: 18.1 mm in April, 7.4 mm in June, 8.5 mm in July 2010, 12.9 mm in October, 15.2 mm in December 2011, and 15.1 mm in February 2012 (Fig. 7).

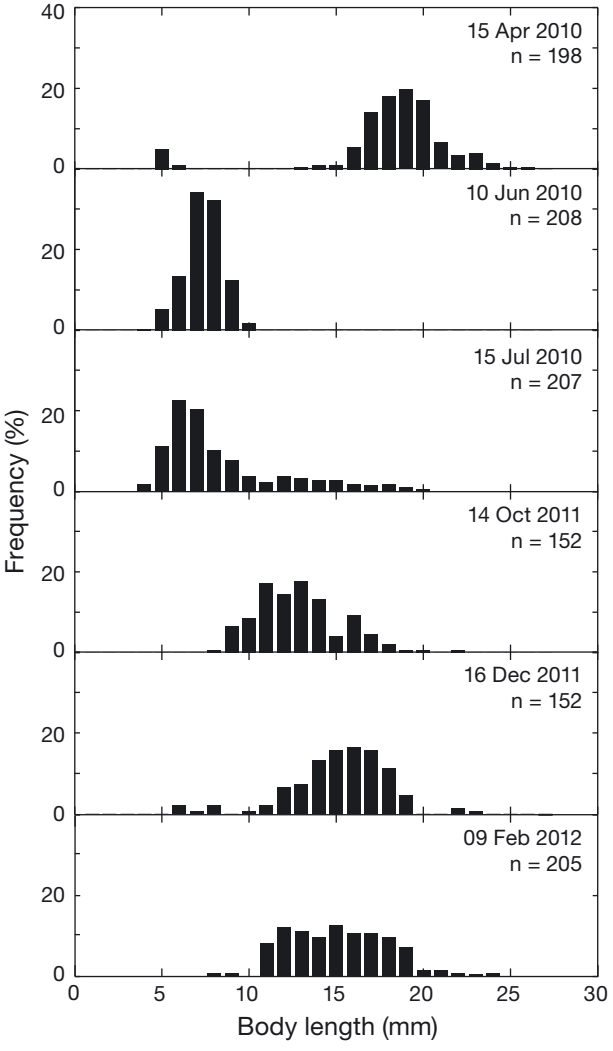

Fig. 7. Size distribution of euphausiids (mostly *Euphausia pacifica*) collected from the surface scattering layers during April, June, July 2010, October, December 2011, and February 2012. n = individuals counted

Migration speed

Since we base our migration timings on near-surface signals, migration speed can affect the dusk arrival timing near the surface. Seasonally averaged migration speeds at dusk ascent/dawn descent are 2.0/2.1 cm s^{-1} during spring, 2.7/1.6 cm s^{-1} during summer, 3.0/2.3 cm s^{-1} during fall, and 2.0/1.5 cm s^{-1} during winter. Because the histograms of lag in migration timing, but not velocities, have normal distributions, the statistical significance of mean lag times between seasons is examined. There are no significant differences ($p > 0.05$) in dusk ascent mean lag time during spring and winter, or during summer and fall. Similarly, there are no significant differences ($p > 0.05$) in dawn descent mean lag time during spring and fall, or during summer and winter. Significant differences ($p < 0.05$) in mean lag times were observed in other seasons. If migration speed were a major cause of the late dusk ascent timing during winter, significant differences in dusk ascent mean lag times during winter and spring–fall would be expected. Since dusk ascent mean lag time during winter is not significantly different from spring, migration speed is unlikely a cause of the seasonal variability in migration timing and not considered further.

DISCUSSION

Summary

The goal of this study was to characterize second-order variability in migration timing relative to civil twilight times, and to identify factors regulating this variability. To address this goal, we used an upward-looking echosounder mooring to monitor the migrating scattering layer, a fluorometer to measure chl *a* concentration near the surface to estimate the shadow effect of phytoplankton, and an insolation record. In addition, 6 sampling campaigns for zooplankton were conducted to confirm the identity of animals dominating the scattering layer and characterize their size distribution with season. The primary results in this study are:

(1) Migration timing of euphausiids exhibits second-order variability at seasonal timescales; early dusk ascent is associated with late dawn descent during spring–fall, and late dusk ascent is associated with early dawn descent during winter.

(2) Ascent timing appears to be controlled by a combination of shadowing by phytoplankton blooms

and the seasonal change in the average body size of euphausiids affecting the phototaxis behavior.

(3) Descent timing appears to be controlled by the seasonal change in the average body size of euphausiids, which affects phototactic behavior.

(4) These results support the size-dependent migration timing hypothesis (De Robertis et al. 2000), whereby more visually conspicuous larger-bodied euphausiids enter surface waters later and leave earlier than smaller-bodied individuals, with a 2-yr time-series covering a life cycle of the dominant euphausiids *Euphausia pacifica*.

Factors affecting diel vertical migration timing

Light is the major control of diel vertical migration timing. Both the absolute and relative rate of change in light intensity have been reported to initiate migration (reviewed by Cohen & Forward 2009). However, these effects could not be examined directly in the present study because the sensitivity of the irradiance sensor was too low to measure insolation before/after civil twilight times. Instead, we consider the following factors that can affect either underwater light intensity or phototactic behaviors of diel vertical migration and thus may regulate the observed second-order seasonal variability in migration timing: (1) shadowing by phytoplankton blooms, (2) food availability, (3) predator density, and (4) zooplankton body size (Table 1).

Shadowing by phytoplankton blooms

Changes in light attenuation due to phytoplankton blooms can affect diel vertical migratory behavior. Kaartvedt et al. (1996) reported that euphausiids and mesopelagic fish ascended by ~100 m during the day during periods of decreased light penetration associated with increased chlorophyll concentrations. Similarly, Frank & Widder (2002) found that the daytime depth of euphausiids shoaled by >100 m during an influx of turbid water relative to their depth before or after the turbidity event. In a very productive ecosystem like Saanich Inlet, high concentrations of phytoplankton in spring–summer inhibit light penetration (Fig. 6), reducing light intensity at 20 m depth to levels comparable to winter conditions (Watanabe 1978).

Although phytoplankton shadowing is evident in Saanich Inlet, the daytime depth of the euphausiid scattering layer is unlikely to be affected because the oxycline determines their maximum daytime depth. However, it is still possible that phytoplankton shadowing could affect the timing of departure from the daytime depth contributing to the observed seasonal variability in dusk ascent migration timing. Assuming that migration timing is controlled by absolute light intensity, zooplankton may depart their daytime depth earlier during spring–fall (i.e. when phytoplankton are abundant) because light intensity falls below the threshold level earlier. Conversely, during winter, light intensity at the daytime depth is stronger (even with the low insolation) due to the lack of phytoplankton, thereby possibly delaying

Table 1. Possible factors affecting second-order seasonal variability in diel vertical migration timing. Each factor has an effect (+)/no effect (–) on dusk ascent and dawn descent migration timings. Ascent: arrival at surface; Descent: departure from surface. N/A: factor is not applicable for the present study

Factors	Previously observed/proposed mechanisms (References)	Present study		
		Ascent	Descent	Exceptions
Shadowing by phytoplankton blooms	Shadow effect of phytoplankton changes underwater light intensity (Kaartvedt et al. 1996, Frank & Widder 2002)	+	–	Spring–fall when chl *a* is low
Food availability	Response to light stimulus and duration at surface are modified by food concentration (Huntley & Brooks 1982, Johnsen & Jacobsen 1987, Pearre 2003, Van Gool & Ringelberg 2003)	N/A	N/A	–
Predator density	Response to light stimulus is modified by chemical cues released by predators (Forward & Rittschof 2000, Cohen & Forward 2005)	N/A	N/A	–
Body size	Larger-bodied zooplankton ascend later, and descend earlier than smaller ones to minimize risk of visual predation (De Robertis et al. 2000)	+	+	Pre-spawning period (Feb–Apr)

departure from the daytime depth. These expectations are consistent with the observed early dusk ascent during spring–fall and late ascent during winter. This phytoplankton shadowing effect assumes that the vertical distribution of phytoplankton is similar at dusk as it is during the day, which seems likely given that centric diatoms (which lack locomotory structures) dominate blooms in Saanich Inlet (Takahashi et al. 1978, Grundle et al. 2009). Another assumption is that the daytime depth of the euphausiid scattering layer is constant across seasons, which could not be verified due to the echosounder being deployed shallower than the daytime scattering layer depth. However, it is unlikely a cause of delayed arrival near the surface during winter because the upward movement of the scattering layer associated with oxygen renewal events in fall (Anderson & Devol 1973, Manning et al. 2010) should decrease the migration distance.

Food availability

The phototactic response of zooplankton can be modified by food availability. When exposed to low food concentrations, *Daphnia* spp. show an increased phototactic response to decreasing light intensity (Van Gool & Ringelberg 2003), triggering early ascent. Their response to an increase in relative rate of change in light intensity increases with food concentration (Van Gool & Ringelberg 1995), predicting that well-fed animals will more readily descend at sunrise (Pearre 2003). This hunger-satiation hypothesis is also supported by euphausiid species; the continuing downward movement of fed euphausiids *Meganyctiphanes norvegica* and *Thysanoessa rachii* was observed soon after the ascent (Sourisseau et al. 2008). Therefore, time spent in upper layers can be minimized when food availability is high, whereas zooplankton spend more time near the surface when food availability is low (e.g. Huntley & Brooks 1982, Johnsen & Jacobsen 1987). This hypothesis could be the case in the present study, since winter nights are considerably longer than summer nights, more than compensating for the late dusk ascent and early dawn descent during winter. However, our data show no correlation between migration timings and chl *a* concentration. One difficulty is that the depth of the chlorophyll maximum varies between 5 and 20 m in Saanich Inlet and is not always detected by the fluorometer positioned at a single depth. In addition, euphausiids can switch their diets among phytoplankton, microzooplankton, and suspended organic matter (Mauchline & Fisher 1969, Dilling et al. 1998, Nakagawa et al. 2001, Pinchuk & Hopcroft 2007), so chl *a* concentration is only a proxy of food availability. Thus, the effect of food availability on migration timings remains inconclusive.

Predator density

Phototactic responses can be modified by chemical cues exuded by predators (i.e. kairomones). In the coastal copepod *Calanopia americana*, the threshold of relative rate of change in light intensity to induce an ascent increases in the presence of kairomones (Cohen & Forward 2005), suggesting later ascent when predator abundance is high. Similarly, the photoresponse threshold required to initiate descent in larvae of the estuarine crab *Rhithropanopeus harrisii* decreases in the presence of kairomones (Forward & Rittschof 2000), resulting in an earlier descent of larvae at sunrise to lower their predation risk. Euphausiids are common prey items for planktivorous fish in Saanich Inlet (Bary et al. 1962, Mauchline 1980, Mackas et al. 1997). Adult migratory stocks of Pacific herring move into the Strait of Georgia from November until early March before spawning (Haist & Stocker 1985), and some likely enter Saanich Inlet. Juvenile coho salmon also migrate from the lower Fraser River and Puget Sound into Saanich Inlet by July and August (Holtby et al. 1992). Fish predation pressure therefore varies seasonally due to different species spawning and moving into Saanich Inlet, as well as ontogenic shifts in their diets (Holtby et al. 1992, Adams et al. 2007). Although predation risk likely plays some role in regulating the second-order variability in migration timing, quantification of predator density could not be explored in our study (see 'Data analysis: Application of threshold' above).

Zooplankton body size

Size-dependent migration timing to avoid visual predators contributes to the observed seasonal variability in both dusk ascent and dawn descent migration timings; larger euphausiids during winter ascend later and descend earlier than smaller individuals during summer (Figs. 4 & 7). In Saanich Inlet, juvenile *Euphausia pacifica* ascend as much as 30 min earlier and descend up to 45 min later than adults (De Robertis et al. 2000). Size-dependent migration timing can explain the observed seasonal variability between summer and winter when the

euphausiid population is dominated by different size classes (Fig. 7). However, early dusk ascent and late dawn descent during late February to April cannot be explained by this hypothesis, since the population is dominated by adults at this time. One possible explanation is the energy demand related to the euphausiid reproduction cycle. Summer is a period of intense spawning activity for *E. pacifica* (Parsons et al. 1967, Heath 1977). Ovarian development and maturation occur over a period of several months prior to spawning (Ross & Quetin 2000) and euphausiids invest large amounts of energy into reproduction (Virtue et al. 1996, Shaw et al. 2010). Tarling (2003) observed that the greater energy demand required to fuel reproduction appears to drive females to riskier diel vertical migration than males in the northern krill *Meganyctiphanes norvegica*. High energy demand for reproduction can thus result in early dusk ascent and late dawn descent to maximize time spent at the food-rich surface during phytoplankton blooms.

More complicated diel vertical migration patterns

Multiple small targets and fewer large targets can result in similar S_v values, because a single-frequency echosounder only measures S_v and cannot distinguish individuals. Thus, our migration-timing detection assumes the arrival/departure of a single scattering layer (dominated by euphausiids) at/from the surface. However, our 2-yr echosounder time-series also reveals more highly variable and complex patterns, including 2-layer upward migration where 2 layers migrate parallel to each other (Fig. 8a) or a single scattering layer diverges into 2 or 3 layers

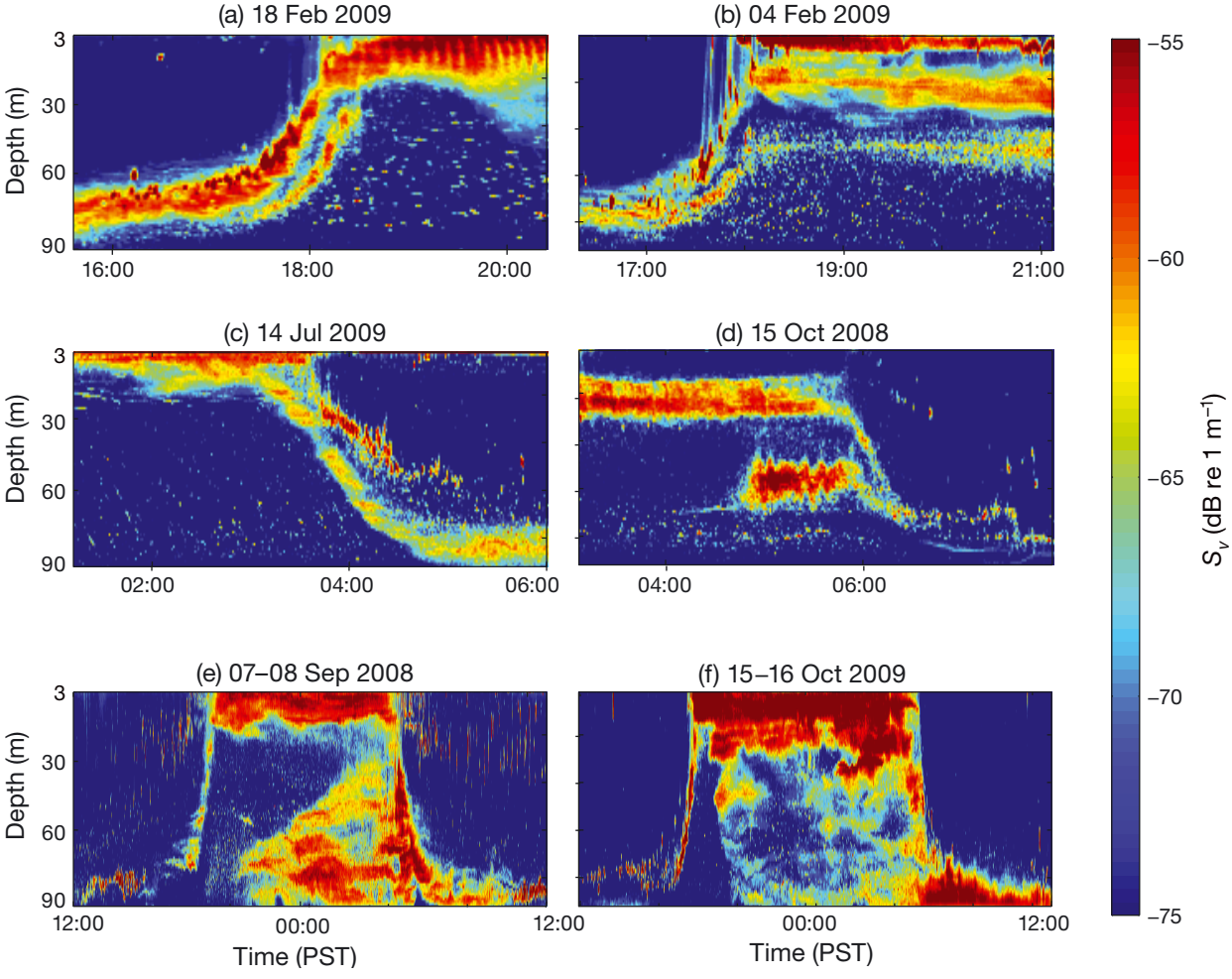

Fig. 8. Sample echograms of volume backscattering strength (S_v) (1-min × 1-m bin averages), showing more complicated diel vertical migration patterns including (a,c) 2 layer, (b) divergence, (d) convergence, (e) partial upward, and (f) partial downward migrations

(Fig. 8b); 2-layer downward migration where a scattering layer diverges into 2 layers (Fig. 8c) or 2 layers converge into 1 (Fig. 8d); and partial upward (Fig. 8e) or downward (Fig. 8f) migrations. Establishing a classification scheme of these complex patterns proved difficult due to the presence of confusing migration patterns, variability in thickness and strength of the scattering layers, as well as changes in spatial and temporal separations of multiple scattering layers. The occurrence of these patterns was examined in relation to seasonality, tidal cycle, moon phases and cloud cover, but no clear correlation was found. We suggest that such complex migration patterns are likely comprised of multiple species or multiple life history stages of a single species. They may be regulated by the feeding success of the migrators (Pearre 2003). For example, a 2-layer migration pattern (similar to Fig. 8a) comprised of the euphausiid *Meganyctiphanes norvgica* and pteropod *Cavoliania inflexa* in discrete bands was observed in the Ligurian Sea (Tarling et al. 2001). A large fraction of the population of *Calanus pacificus* females did not migrate into the surface layer at night, but stayed below the chlorophyll maximum in the 25–50 m range in Dabob Bay, Washington (Dagg et al. 1997). Sourisseau et al. (2008) observed the continuing downward movement of fed euphausiids *M. norvegica* and *Thysanoessa raschii* soon after the ascent in the St. Lawrence Estuary. Understanding complex migration structures requires tracking not only mass transfer but also the interchange of individuals, which is beyond the scope of the present study.

CONCLUSIONS

We conclude that a combination of phytoplankton bloom shadowing and the seasonal cycle in average euphausiid body size affect phototaxis behavior determining dusk ascent timing. Seasonal variability in dawn descent timing is most likely regulated by euphausiid body size. It is tempting to suppose that the seasonal correspondence in lags between dusk ascent and dawn descent migration timings (Fig. 3d) suggests a common driving mechanism. However, previous studies suggest that the photobiological control of diel vertical migration behavior may differ between the ascent and descent phases within a species (Forward et al. 1984, Forward 1985). Our observations suggest that phytoplankton concentration can have higher impact on determining light intensity at daytime depth of the scattering layer than insolation, and likely affects dusk ascent timing. Our 2-yr time-series also supports the size-dependent migration timing hypothesis (De Robertis et al. 2000), whereby more visually conspicuous larger-bodied euphausiids enter surface waters later and leave earlier than smaller-bodied individuals. However, the pre-spawning period may be an exception to this hypothesis; rather than minimizing visual predation risk, migration timing may be timed to maximize energy gain. The hunger-satiation hypothesis could not be addressed in this study, because we did not include variability in migration timing other than dusk and dawn such as midnight sinking. Instead of the traditional view of diel vertical migration timing, which is only correlated with civil twilight, our data suggest that euphausiids also adapt their migration timings seasonally to accommodate changes in environmental cues as well as their growth pattern.

Acknowledgements. We thank G. Borstad for his suggestion of applying the 3D data cube concept to the echosounder data. The manuscript was greatly improved through the discussion with J. Klymak. The staff of the VENUS cabled observatory assisted with accessing the echosounder data. D. Lemon and M. Clarke provided the technical support for calibrating echosounders, and A. Proctor helped us access the buoy of the Ocean Technology Test Bed for calibrations. We thank J. Horne for his advice on calibration analysis. J. Gower provided the chl a data from MEOS buoy, E. Wiebe provided the insolation data from the University of Victoria's school-based weather station network, and S. Thornton provided CTD data collected in Saanich Inlet during 2007–2011. Field support was provided by Captain K. Brown and the crew of MSV 'John Strickland', with the help of I. Beveridge, L. Guan, K. Sorochan, J. Rose, D. Bevan, E. Murowinski and K. Bartlett. We thank D. Mackas, S. Kaartvedt and 3 anonymous reviewers for their valuable comments to improve the manuscript. This work was supported by US Office of Naval Research N0000140810700 and NSERC Discovery Grants to E.K. and J.F.D. Additionally, M.S. was supported by the Bob Wright Scholarship.

LITERATURE CITED

Adams CF, Pinchuk AI, Coyle KO (2007) Seasonal changes in the diet composition and prey selection of walleye pollock (*Theragra chalcogramma*) in the northern Gulf of Alaska. Fish Res 84:378–389

Anderson JJ, Devol AH (1973) Deep water renewal in Saanich Inlet, an intermittently anoxic basin. Estuar Coast Mar Sci 1:1–10

Bary BM (1966) Backscattering at 12 kc/s in relation to biomass and numbers of zooplanktonic organisms in Saanich Inlet, British Columbia. Deep-Sea Res 13:655–666

Bary BM, Barraclough WE, Herlinveaux R (1962) Scattering of underwater sound in Saanich Inlet, British Columbia. Nature 194:36–37

Blaxter JHS (1973) Monitoring the vertical movements and light responses of herring and plaice larvae. J Mar Biol Assoc UK 53:635–647

Bollens SM, Frost BW (1989) Zooplanktivorous fish and variable diel vertical migration in the marine planktonic copepod *Calanus pacificus*. Limnol Oceanogr 34: 1072–1083

Borstad G, Brown L, Sato M, Lemon D, Kerr R, Willis P (2010) Long zooplankton time series with high temporal and spatial resolution. MTS/IEEE Int Conf Oceans 2010, doi:10.1109/OCEANS.2010.5664585

Cisewski B, Strass VH, Rhein M, Krägefsky S (2010) Seasonal variation of diel vertical migration of zooplankton from ADCP backscatter time series data in the Lazarev Sea, Antarctica. Deep-Sea Res I 57:78–94

Cohen JH, Forward RB (2005) Photobehavior as an inducible defense in the marine copepod *Calanopia americana*. Limnol Oceanogr 50:1269–1277

Cohen JH, Forward RB (2009) Zooplankton diel vertical migration: a review of proximate control. Oceanogr Mar Biol Annu Rev 47:77–109

Dagg MJ, Frost BW, Newton JA (1997) Vertical migration and feeding behavior of *Calanus pacificus* females during a phytoplankton bloom in Dabob Bay, US. Limnol Oceanogr 42:974–980

De Robertis A (2001) Validation of acoustic echo counting for studies of zooplankton behavior. ICES J Mar Sci 58: 543–561

De Robertis A (2002) Small-scale spatial distribution of the euphausiid *Euphausia pacifica* and overlap with planktivorous fishes. J Plankton Res 24:1207–1220

De Robertis A, Jaffe JS, Ohman MD (2000) Size-dependent visual predation risk and the timing of vertical migration in zooplankton. Limnol Oceanogr 45:1838–1844

Devol AH (1981) Vertical distribution of zooplankton respiration in relation to the intense oxygen minimum zones in two British Columbia fjords. J Plankton Res 3:593–602

Dilling L, Wilson J, Steinberg D, Alldredge A (1998) Feeding by the euphausiid *Euphausia pacifica* and the copepod *Calanus pacificus* on marine snow. Mar Ecol Prog Ser 170:189–201

Faran JJ (1951) Sound scattering by solid cylinders and spheres. J Acoust Soc Am 23:405–418

Foote KG (1982) Optimizing copper spheres for precision calibration of hydroacoustic equipment. J Acoust Soc Am 71:742–747

Forward RB (1985) Behavioral responses of larvae of the crab *Rhithropanopeus harrisii* (Brachyura: Xanthidae) during diel vertical migration. Mar Biol 90:9–18

Forward RB (1988) Diel vertical migration: zooplankton photobiology and behaviour. Oceanogr Mar Biol Annu Rev 26:361–393

Forward RB, Rittschof D (2000) Alteration of photoresponses involved in diel vertical migration of a crab larva by fish mucus and degradation products of mucopolysaccharides. J Exp Mar Biol Ecol 245:277–292

Forward RB, Cronin TW, Stearns DE (1984) Control of diel vertical migration: photoresponses of a larval crustacean. Limnol Oceanogr 29:146–154

Francois RE, Garrison GR (1982) Sound absorption based on ocean measurements. Part II: boric acid contribution and equation for total absorption. J Acoust Soc Am 72: 1879–1890

Frank TM, Widder EA (1999) Comparative study of the spectral sensitivities of mesopelagic crustaceans. J Comp Physiol A 185:255–265

Frank TM, Widder EA (2002) Effects of a decrease in downwelling irradiance on the daytime vertical distribution patterns of zooplankton and micronekton. Mar Biol 140: 1181–1193

Gargett AE, Stucchi D, Whitney F (2003) Physical processes associated with high primary production in Saanich Inlet, British Columbia. Estuar Coast Shelf Sci 56:1141–1156

Gower JFR (2001) Productivity and plankton blooms observed with Seawifs and *in situ* sensors. Int Geosci Remote Sens Symp, IEEE 5:2181–2183

Gower J, Peña A, Gargett A (1999) Biological monitoring with the western Canadian ODAS marine buoy network. OCEANS '99 MTS/IEEE 3:1244–1248

Grundle DS, Timothy DA, Varela DE (2009) Variations of phytoplankton productivity and biomass over an annual cycle in Saanich Inlet, a British Columbia fjord. Cont Shelf Res 29:2257–2269

Haist V, Stocker M (1985) Growth and maturation of Pacific herring (*Clupea harengus pallasi*) in the Strait of Georgia. Can J Fish Aquat Sci 42:138–146

Heath WA (1977) The ecology and harvesting of euphausiids in the Strait of Georgia. PhD thesis, University of British Columbia, Vancouver

Herlinveaux RH (1962) Oceanography of Saanich Inlet in Vancouver Island, British Columbia. J Fish Res Board Can 19:1–37

Hickling R (1962) Analysis of echoes from a solid elastic sphere in water. J Acoust Soc Am 34:1582–1592

Holliday DV, Pieper RE (1995) Bioacoustical oceanography at high frequencies. ICES J Mar Sci 52:279–296

Holtby LB, Kadowaki RK, Simpson KS (1992) Factor affecting the vulnerability of juvenile coho (*Oncorhynchus kisutch*) and chinook salmon (*O. tshawytscha*) in a saltwater sport fishery. Can J Fish Aquat Sci 49:2164–2178

Hulburt EO (1945) Optics of distilled and natural water. J Opt Soc Am 35:698–705

Huntley M, Brooks ER (1982) Effects of age and food availability on diel vertical migration of *Calanus pacificus.* Mar Biol 71:23–31

Jaffe JS, Ohman MD, De Robertis A (1998) OASIS in the sea: measurement of the acoustic reflectivity of zooplankton with concurrent optical imaging. Deep-Sea Res II 45: 1239–1253

Jiang S, Dickey TD, Steinberg DK, Madin LP (2007) Temporal variability of zooplankton biomass from ADCP backscatter time series data at the Bermuda Testbed Mooring site. Deep-Sea Res I 54:608–636

Johnsen GH, Jacobsen PJ (1987) The effect of food limitation on vertical migration in *Daphnia longispina*. Limnol Oceanogr 32:873–880

Kaartvedt S, Melle W, Knutsen T, Skjoldal HR (1996) Vertical distribution of fish and krill beneath water of varying optical properties. Mar Ecol Prog Ser 136:51–58

Longhurst AR, Harrison WG (1988) Vertical nitrogen flux from the oceanic photic zone by diel migrant zooplankton and nekton. Deep-Sea Res A 35:881–889

Lorke A, McGinnis DF, Spaak P, Wüest A (2004) Acoustic observations of zooplankton in lakes using a Doppler current profiler. Freshw Biol 49:1280–1292

Mackas DL, Kieser R, Saunders M, Yelland DR, Brown RM, Moore DF (1997) Aggregation of euphausiids and Pacific hake (*Merluccius productus*) along the outer continental shelf off Vancouver Island. Can J Fish Aquat Sci 54: 2080–2096

Mackenzie KV (1981) Nine-term equations for sound speed in the oceans. J Acoust Soc Am 70:807–812

Mackie GO, Mills CE (1983) Use of the *Pisces IV* sub-

mersible for zooplankton studies in coastal waters of British Columbia. Can J Fish Aquat Sci 40:763–776

MacLennan DN, Dunn JR (1984) Estimation of sound velocities from resonance measurements on tungsten carbide calibration spheres. J Sound Vibrat 97:321–331

Manning CC, Hamme RC, Bourbonnais A (2010) Impact of deep-water renewal events on fixed nitrogen loss from seasonally-anoxic Saanich Inlet. Mar Chem 122:1–10

Mauchline J (1980) The biology of mysids and euphausiids. Adv Mar Biol 18:1–681

Mauchline J, Fisher LR (1969) The biology of euphausiids. Adv Mar Biol 7:1–454

Nakagawa Y, Endo Y, Taki K (2001) Diet of *Euphausia pacifica* Hansen in Sanriku waters off northeastern Japan. Plankton Biol Ecol 48:68–77

Ona E (1999) Methodology for target strength measurements. ICES Coop Res Rep 235:49–59

Parsons TR, Lebrasseur RJ, Fulton JD (1967) Some observations on the dependence of zooplankton grazing on the cell size and concentration of phytoplankton blooms. J Oceanogr Soc Jpn 23:10–17

Pearre S (2003) Eat and run? The hunger/satiation hypothesis in vertical migration: history, evidence and consequences. Biol Rev Camb Philos Soc 78:1–79

Pieper RE (1971) A study of the relationship between zooplankton and high-frequency scattering of underwater sound. PhD thesis, University of British Columbia, Vancouver

Pinchuk A, Hopcroft RR (2007) Seasonal variations in the growth rates of euphausiids (*Thysanoessa inermis, T. spinifera*, and *Euphausia pacifica*) from the northern Gulf of Alaska. Mar Biol 151:257–269

Proctor AA, Bradley C, Gamroth E, Kennedy J (2007) The Ocean Technology Test Bed: an underwater laboratory. MTS/IEEE Int Conf Oceans 2007, doi:10.1109/OCEANS.2007.4449178

Ross RM, Quetin L (2000) Reproduction in Euphausiacea. In: Everson I (ed) Krill: biology, ecology and fisheries. Blackwell Science, Oxford, p 150–181

Sato M, Jumars PA (2008) Seasonal and vertical variations in emergence behaviors of *Neomysis americana*. Limnol Oceanogr 53:1665–1677

Shaw CT, Peterson WT, Feinberg LR (2010) Growth of *Euphausia pacifica* in the upwelling zone off the Oregon coast. Deep-Sea Res II 57:584–593

Simard Y, Lactoix G, Legendre L (1985) *In situ* twilight grazing rhythm during diel vertical migrations of a scattering layer of *Calanus finmarchicus*. Limnol Oceanogr 30:598–606

Sourisseau M, Simard Y, Saucier FJ (2008) Krill diel vertical migration fine dynamics, nocturnal overturns, and their roles for aggregation in stratified flows. Can J Fish Aquat Sci 65:574–587

Stanton TK, Wiebe PH, Chu D, Benfield MC, Scanlon L, Martin L, Eastwood RL (1994) On acoustic estimates of zooplankton biomass. ICES J Mar Sci 51:505–512

Stanton TK, Chu D, Wiebe PH (1996) Acoustic scattering characteristics of several zooplankton groups. ICES J Mar Sci 53:289–295

Steinberg DK, Carlson CA, Bates NR, Goldthwait SA, Madin LP, Michaels AF (2000) Zooplankton vertical migration and the active transport of dissolved organic and inorganic carbon in the Sargasso Sea. Deep-Sea Res I 47:137–158

Takahashi M, Barwell-Clarke J, Whitney F, Koeller P (1978) Winter condition of marine plankton populations in Saanich Inlet, BC, Canada. I. Phytoplankton and its surrounding environment. J Exp Mar Biol Ecol 31:283–301

Tanasichuk RW (1998) Interannual variations in the population biology and productivity of *Euphausia pacifica* in Barkley Sound, Canada, with special reference to the 1992 and 1993 warm ocean years. Mar Ecol Prog Ser 173:163–180

Tarling GA (2003) Sex-dependent diel vertical migration in northern krill *Meganyctiphanes norvegica* and its consequences for population dynamics. Mar Ecol Prog Ser 260:173–188

Tarling GA, Matthews JBL, David P, Guerin O, Buchholz F (2001) The swarm dynamics of northern krill (*Meganyctiphanes norvegica*) and pteropods (*Cavolinia inflexa*) during vertical migration in the Ligurian Sea observed by an acoustic Doppler current profiler. Deep-Sea Res I 48:1671–1686

Timothy DA, Soon MYS (2001) Primary production and deep-water oxygen content of two British Columbian fjords. Mar Chem 73:37–51

Trevorrow MV (2005) The use of moored inverted echo sounders for monitoring meso-zooplankton and fish near the ocean surface. Can J Fish Aquat Sci 62:1004–1018

Tyler JE (1975) The *in situ* quantum efficiency of natural phytoplankton populations. Limnol Oceanogr 20:976–980

Urick RJ (1983) Principles of underwater sound. McGraw Hill, New York, NY

Vagle S, Foote KG, Trevorrow MV, Farmer DM (1996) A technique for calibration of monostatic echosounder systems. IEEE J Oceanic Eng 21:298–305

Van Gool E, Ringelberg J (1995) Swimming of *Daphnia galeata* × *hyalina* in response to changing light intensities: influence of food availability and predator kairomone. Mar Freshw Behav Physiol 26:259–265

Van Gool E, Ringelberg J (2003) What goes down must come up: symmetry in light-induced migration behaviour of *Daphnia*. Hydrobiologia 491:301–307

Virtue P, Nichols PD, Nicol S, Hosie G (1996) Reproductive trade-off in male Antarctic krill, *Euphausia superba*. Mar Biol 126:521–527

Watanabe LN (1978) Factors controlling the winter dominance of nanoflagellates in Saanich Inlet, British Columbia. MSc thesis, University of British Columbia, Vancouver

Widder EA, Frank TM (2001) The speed of an isolume: a shrimp's eye view. Mar Biol 138:669–677

Zaret TM, Suffern JS (1976) Vertical migration in zooplankton as a predator avoidance mechanism. Limnol Oceanogr 21:804–813

Appendix 1. Calibrations

Both echosounders were calibrated using the target strength (TS) of a 38.1 mm diameter tungsten carbide reference sphere as prescribed by Vagle et al. (1996). The equation used in the AWCP systems for estimating TS measured *in situ* was:

$$TS = 20\log_{10} N_r + 40\log_{10} r + 2\alpha r - SL - OCV - G \quad (A1)$$

System calibrations for TS measurements involve guiding the sphere through the beam, measuring its TS, and quantifying adjustment needed in G to compensate for the difference between the TS measured *in situ* and theoretical TS of the sphere as ΔG. The theoretical TS values of the reference sphere were computed for the center frequency and bandwidth of each echosounder (Faran 1951, Hickling 1962, Foote 1982).

Calibrations were conducted at the buoy of the Ocean Technology Test Bed, an underwater engineering laboratory operated by the University of Victoria in Saanich Inlet (Proctor et al. 2007), on 9 February 2010 for AWCP 1007 and 31 January 2011 for AWCP 1009. Due to technical difficulties in calibrating bottom-mounted echosounders at the operating depth of 100 m, calibrations were conducted near the surface. The calibration system consists of a simple assembly, with a fixed vertical post attached to the buoy onto which the transducer was mounted at ~0.7 m depth facing downward. A calibration sphere was enmeshed in fine seine woven of monofilament nylon and suspended below the transducer at 20 to 37 m range using monofilament fishing lines. The position of the sphere was controlled vertically and horizontally in order to find the acoustic axis, and the calibration sphere was deepened every 2 to 5 m for calibration measurements at different depths. The AWCP 1007 calibration included 846 TS measurements in 4 different depths averaging 212 TS measurements at each depth. The AWCP 1009 calibration included 1592 TS measurements in 6 different depths averaging 265 TS measurements at each depth. CTD vertical profiles were collected during the calibrations, from which the sound speed (c) was estimated (Mackenzie 1981). The mean c was computed between the depths of the transducer (0.7 m) and sphere (20–37 m); c = 1476 m s^{-1} for AWCP 1007, and c = 1474 m s^{-1} for AWCP 1009. The mean c was used to compute theoretical TS values, as well as r and α (Francois & Garrison 1982). Based on theoretical longitudinal and transverse sound speed of the reference sphere (MacLennan & Dunn 1984) and measured sound speed during calibrations, theoretical TS was –39.51 dB re 1 m^2 for AWCP 1007 and –39.52 dB re 1 m^2 for AWCP 1009.

Although weather during calibration was relatively calm and tides are weak in Saanich Inlet, positioning of the sphere on the acoustic axis was difficult due to the single-beam echosounder. Since the TS value should become maximum when the sphere is located on the acoustic axis, the maximum TS obtained during calibration runs at each depth was taken to be an on-axis measurement and used for calculating ΔG. On average, the mean adjustment needed in G (ΔG) was –0.34 dB for AWCP 1007 and –0.38 dB for AWCP 1009 (Table A1). Since the measured TS values were within 0.4 dB of the theoretical TS and depth dependency of transducer sensitivity could affect the calibration results (Ona 1999), no correction was applied to G in the present study.

Table A1. Calibration values for AWCPs

Serial number of AWCP	1007				1009					
Calibration date	9 February 2010				31 January 2011					
Center frequency (kHz)	201.6				200.4					
SL (dB re 1 µPa at 1m)	212.6				212.9					
OCV (dB re 1 V per 1 µPa)	–191.2				–191.2					
r (m)	22.66	24.69	30.76	36.83	19.46	21.48	23.49	25.53	30.46	35.28
ΔG (dB)	–0.22	0.08	–0.11	–1.10	–0.78	–0.75	–0.82	0.30	–0.21	0.03
Mean ± SD of ΔG (dB)	–0.34 ± 0.52				–0.38 ± 0.47					

Editorial responsibility: Marsh Youngbluth, Fort Pierce, Florida, USA

Submitted: June 25, 2012; Accepted: December 4, 2012
Proofs received from author(s): April 6, 2013